# A Sensitivity Analysis for the Adequacy Assessment of a Multi-State Physics Modeling Approach for Reliability Analysis

Wei Wang & Francesco Di Maio
*Energy Department, Politecnico di Milano, Via La Masa 34, 20156 Milano, Italy*

Enrico Zio
*Energy Department, Politecnico di Milano, Via La Masa 34, 20156 Milano, Italy*

*Chair on System Science and the Energetic Challenge, Fondation EDF-Electricite de France, Ecole Centrale Paris and Supelec, Chatenay-Malabry Cedex, 92295 Paris, France*

ABSTRACT: In this work, a moment-independent Sensitivity Analysis (SA) based on Hellinger distance and Kullback-Leibler divergence is proposed to identify the component of a system most affecting its reliability. This result is used to adequately allocate modeling efforts on the most important component that, therefore, deserves a component-level Multi-State Physics Modeling (MSPM) to be integrated into a system-level model, to estimate the system failure probability. A Reactor Protection System (RPS) of a Nuclear Power Plant (NPP) is considered as case study, wherein the embedded Resistance Temperature Detector (RTD) is identified as the most important component. Results show the benefits of using MSPM to model the RTD with respect to a Markov Chain Model (MCM), because the former gives due account to the aging- and environmental-dependent phenomena that affect the transition rates of the system-level degradation model. In conclusion, the proposed RPS-MSPM can be seen as a trade-off model leveraging accuracy and computational demand.

KEYWORDS: Digital I&C System; Reactor Protection System; Resistance Temperature Detector; Multi-State Physics Modeling; Sensitivity Analysis; Hellinger Distance; Kullback-Leibler Divergence.

## 1 INTRODUCTION

Multi-State Physics Modeling (MSPM) is a semi-Markov modeling approach that can be used in component- or/and system-level reliability assessment, for accounting for the effects of both the stochastic degradation process and the uncertain environmental and operational parameters (Di Maio et al., 2015; Lin et al., 2015; Zio, 2016). MSPM offers the possibility of embedding the physical degradation process into the assessment (Wang et al., 2016).

However, this entails demanding efforts for modeling the physical relationships needed to build the physics-based models and high computational burden for manipulating the large amount of data, especially when treating their uncertainties (Aldemir, 2013; Zio, 2014). As a result, a trade-off choice between modeling accuracy and computational demand is needed for practical reliability assessment based on MSPM of a complex system. In this study, Sensitivity Analysis (SA) is proposed for the assessment of a MSPM, to help the analyst to identify the components of a system that most deserve accurate modeling of aging- and environmental-dependent transition rates, for accurate system reliability assessment. The SA is performed based on moment-independent sensitivity measures, such as Hellinger distance and Kullback-Leibler divergence (Diaconis et al., 1982; Gibbs et al., 2002; Di Maio et al., 2014).

In what follows, Section 2 describes the Reactor Protection System (RPS) of a Nuclear Power Plant (NPP) taken as case study, and its Markov Chain Model (MCM) reliability model taken as reference model. In Section 3, SA in the MCM is performed and the Resistance Temperature Detector (RTD) is identified as the component most affecting the RPS reliability. Section 4, then, shows the best trade-off MSPM model for the system dynamic reliability assessment of the RPS and, in Section 5, some conclusions are drawn.

## 2 THE REACTOR PROTECTION SYSTEM

The objective of RPS is to trigger the NPP emergency shutdown, as soon as an anomaly is detected in the measurements of a relevant signal (here taken to be a temperature signal). As shown in Figure 1, the RPS considered is composed of two redundant channels (A and B). Each channel consists of one signal sensor (S-A and S-B), one Bistable Processor Logic (BPL) subsystem (BPL-A and BPL-B), and one Local Coincidence Logic (LCL) subsystem (LCL-A and LCL-B). It is worth mentioning that given the important role that RTDs play in NPPs digital Instrumentation and Control (I&C) systems (Hashemian, 2011; Yun et al., 2012; Baraldi et al., 2015), we assume S-A and S-B of Figure 1 to be RTDs.

If any of the two redundant measured signals exceeds a triggering threshold value, a Partial Tripping Signal (PTS) is sent to the corresponding

BPL. The signal processing proceeds only if both channels produce the PTS: each PTS from a BPL is sent to both LCL-A and LCL-B, which process information by an "AND" gate. In other words, an Emergency Shutdown Signal (ESS) is produced only when receiving two PTSs from different BPLs; ESSs, then, activates the Reactor Trip Breaker (RTB), when at least one ESS is triggered, i.e., the information is processed by an "OR" gate. Once the RTB is activated, the power supply system and Control Rod Drive Mechanism (CRDM), which are connected with the RTB come into use to control the power of the reactor.

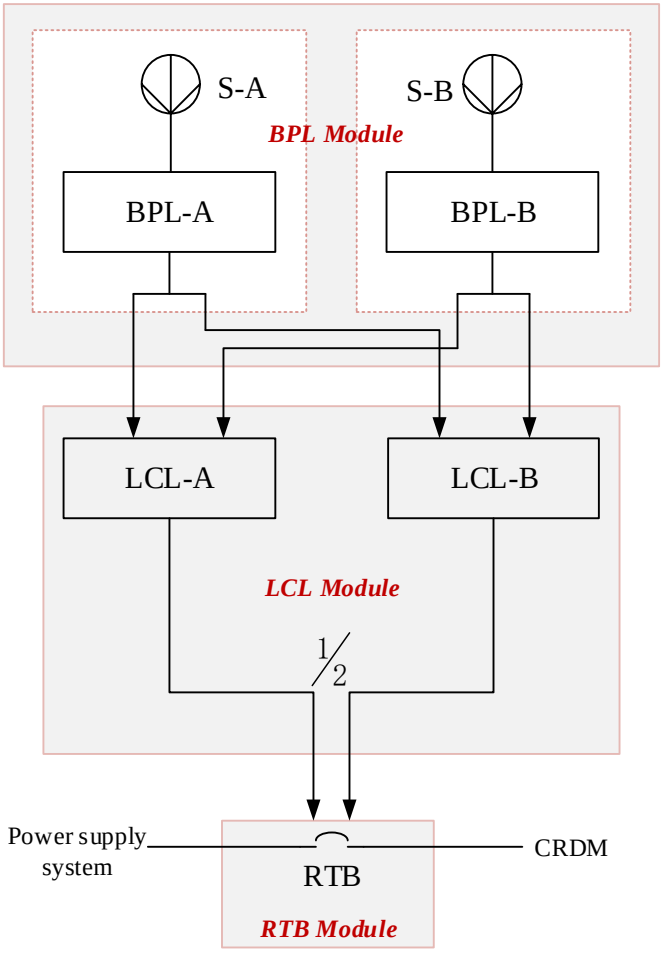


Figure 1. A typical RPS (Wang et al., 2015)

According to the RPS scheme reported in Figure 1, three modules are identified:

- The BPL Module consists of two groups of components: each one being the series of one sensor and BPL (i.e., "S-A and BPL-A" and "S-B and BPL-B").
- The LCL Module consists of the two LCLs (i.e., LCL-A and LCL-B). Since the ESS is triggered only when both LCLs simultaneously receive two PTSs from the two BPLs, this module is highly dependent on the BPL module.
- The RTB Module.

## *2.1 The RPS-MCM*

In this Section, a MCM model is proposed as reference model for the reliability assessment of the RPS. To do this, intra- and inter-module states leading to the system failure are to be identified and modeled. Intra-module states refer to the possible states of the components belonging to the same module, whereas, inter-modules states refer to the states that affect simultaneously components of different modules.

Figure 2 shows the RPS-MCM, whose states are listed in Table 1.

The following assumptions have been made for the subsequent quantitative analysis:

- Transitions can occur from the system functioning state (state 0) to any of the absorbing states of the intra-module states, and from the intermediate state (state 3) to any of the absorbing states of the inter-modules states. The transition rates are assumed to be constant values, taken from public database (US: EPRI, 2008; IAEA, 1992) and reported in Table 2.
- Repair rates are assumed to be equal to 0.

Table 1. Description of the states in RPS-MCM

| State | Description |
|---|---|
| 0 | RPS functioning state. |
| 1 | Either one or the other RTD sensor fails. |
| 2 | Either one or the other BPL fails to send out PTSs. |
| 3 | Either one or the other LCL fails to produce the ESS. |
| 4 | RTB fails during operation. |
| 5 | One LCL has failed and, then, one sensor fails. |
| 6 | One LCL has failed and, then, one BPL fails. |
| 7 | Both LCLs fail to produce the ESS. |
| 8 | One LCL has failed and, then, the RTB fails. |
| 9 | Common cause failure of BPL-A and BPL-B. |
| 10 | Common cause failure of LCL-A and LCL-B. |
| 11 | RPS failure state. |

Table 2. Description of the transition rates in RPS-MCM

| Symbol | Description | Value (/yr) |
|---|---|---|
| $\lambda_S$ | RTD failure rate | 8.760e-1 |
| $\beta$ | Common cause factor | 0.1 |
| $\lambda_{BS}$ | BPL failure rate | 7.884e-3 |
| $\lambda_{LS}$ | LCL failure rate | 3.942e-2 |
| $\lambda_{BC}$ | BPLs common cause failure rate | 8.760e-4 |
| $\lambda_{LC}$ | LCLs common cause failure rate | 4.380e-3 |
| $\lambda_R$ | RTB failure rate | 3.767e-4 |

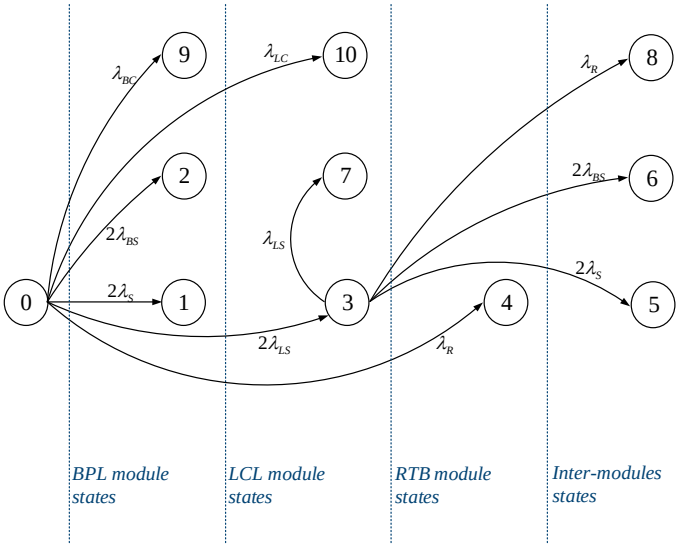


Figure 2. The RPS-MCM model where states are grouped according to their intra-module and inter-modules characteristics.

By the MCM quantitative analysis, the RPS unreliability $P(t)$, its modules unreliabilities $P_{BPL}(t)$, $P_{LCL}(t)$, $P_{RTB}(t)$, and $P_{Inter\text{-}modules}(t)$ are quantified (Figure 3). A visual analysis of the unreliability curves shows that most of the system unreliability $P(t)$ is contributed by the BPL, that is to say, the absorbing states of the BPL module most contribute to the system unreliability.

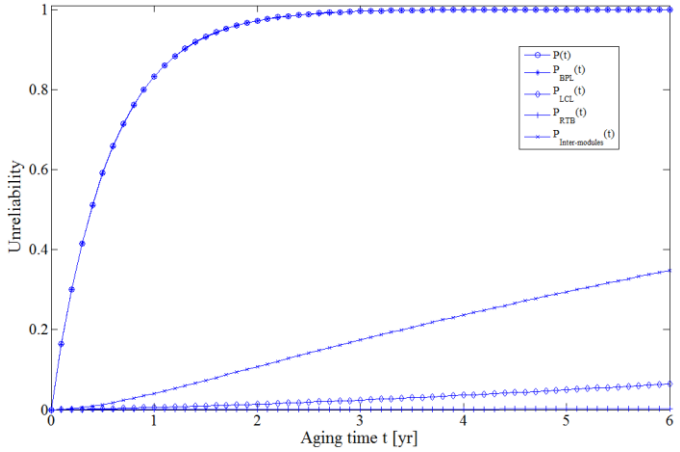


Figure 3. Unreliability curves of RPS and of its modules

## 3 SENSITIVITY ANALYSIS FOR THE IDENTIFICATION OF THE COMPONENT MOST AFFECTING THE RPS RELIABILITY

### *3.1 The SA approach*

The purpose of the analysis is the identification of the component contributing with the largest fraction to the system unreliability. The SA is performed as follows:

1) Calculate a moment-independent measure of the sensitivity of the unreliability $P(t)$ to the unreliability of its $i$-th single contributor $P_i(t)$ (i.e., $P_{BPL}(t)$, $P_{LCL}(t)$, $P_{RTB}(t)$ and $P_{Inter\text{-}modules}(t)$), to identify the most relevant module in the system;
2) Calculate the moment-independent measure for the sensitivity between the module unreliability $P_i(t)$ and the unreliability of its $j$-th embedded component $P_j(t)$, to identify the component most affecting the module unreliability.

The moment-independent sensitivity measures here adopted are the Hellinger distance and Kullback-Leibler divergence (Diaconis et al., 1982; Gibbs et al., 2002; Di Maio et al., 2014). In detail, the Hellinger distance of $H_i[p(t),p_i(t)]$ measures the difference between the pdf $p(t)$ of the system unreliability $P(t)$ and the pdf $p_i(t)$ of the $i$-th contributor to the system failure, i.e., BPL, LCL, RTB, Inter-modules, as follows (Diaconis et al., 1982; Gibbs et al., 2002):

$$H_i\left[p(t),p_i(t)\right]=\left[\frac{1}{2}\int\left(\sqrt{p(t)}-\sqrt{p_i(t)}\right)^2 dt\right]^{\frac{1}{2}}=\left[1-\int\left(\sqrt{p(t)\cdot p_i(t)}\right)^2 dt\right]^{\frac{1}{2}} \quad (1)$$

where the $i$-th contributor is important if $H_i$ is small.

On the other hand, the Kullback-Leibler divergence $KL_i[p(t),p_i(t)]$ measures the different information carried by the pdf $p(t)$ of the system failure and the pdf $p_i(t)$ of the $i$-th contributor as follows (Diaconis et al., 1982; Gibbs et al., 2002):

$$KL_i\left(p(t),p_i(t)\right)=\int_{-\infty}^{+\infty}p(t)\log\left(\frac{p(t)}{p_i(t)}\right)dt \quad (2)$$

with values in [0, + ∞ ]. In practical cases, the symmetric form of Kullback-Leibler divergence can be utilized as follows (Kullback et al., 1951):

$$KL_{sym,i}\left[p(t),p_i(t)\right]=KL_{sym,i}\left[p_i(t),p(t)\right]$$
$$=\frac{1}{2}KL_i\left[p(t),p_i(t)\right]+\frac{1}{2}KL_i\left[p_i(t),p(t)\right] \quad (3)$$

where the $i$-th contributor is important if $KL_{sym,i}$ is small, in relative terms.

### *3.2 Results*

Table 3 lists the Hellinger distance and Kullback-Leibler divergence values for each contributor to the system unreliability, respectively. As suggested by Figure 3, both measures identify the BPL as the most important contributor (see Figures 4 and 5).

Table 3. Ranking of contributors to the RPS unreliability

| Contributor | $H_i$ | $KL_{sym,i}$ |
|---|---|---|
| BPL module | 0.0013 | 6.4539e-6 |
| LCL module | 0.6398 | 2.4181 |
| RTB module | 0.6872 | 3.7300 |
| Inter-modules | 0.6000 | 1.8809 |

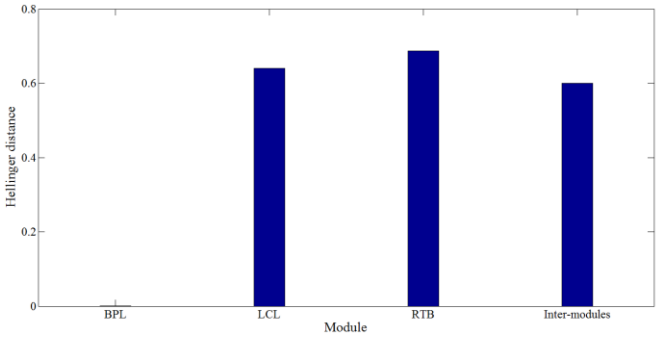


Figure 4. Hellinger distance between the system unreliability curve and of its contributors

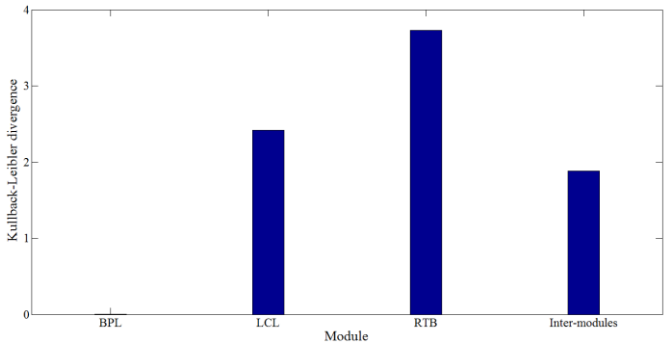


Figure 5. Kullback-Leibler divergence between the system unreliability curve and of its contributors

Since the BPL module plays the most significant role in affecting the reliability of the RPS, we now focus on identifying the BPL-embedded component most contributing to its failure. Figure 6 shows the unreliability of the BPL module and of the components therein embedded (i.e., $P_S(t)$ for the sensor and $P_B(t)$ for the BPL-component).

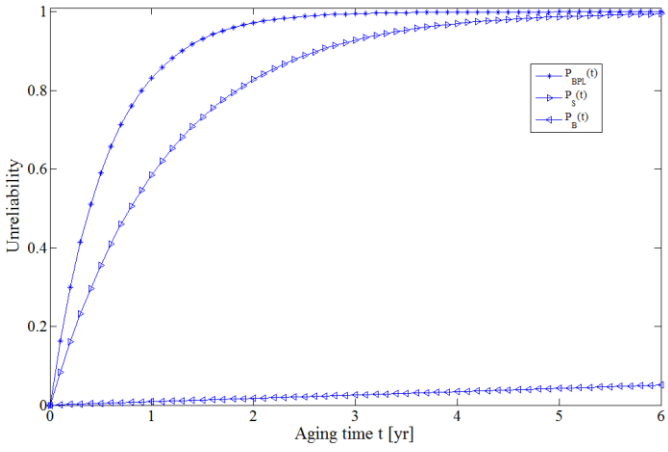


Figure 6. Unreliability of the BPL module and of its embedded components

To rank the importance of the $j$-th component embedded in the BPL module, the two SA measures of Eqs. (1) and (3) are quantified. The sensors turn out to be the most important components contributing to the BPL module unreliability (see Table 4, Figures 7 and 8).

Table 4. Ranking of the contributors to the BPL unreliability

| Input | $H_j$ | $KL_{sym,j}$ |
|---|---|---|
| Sensors | 0.2391 | 0.2460 |
| BPLs | 0.6219 | 2.1599 |

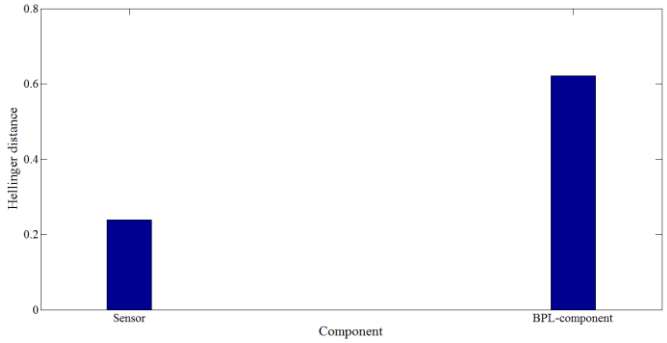


Figure 7. Hellinger distance between the unreliability curve of the BPL module and of its embedded components

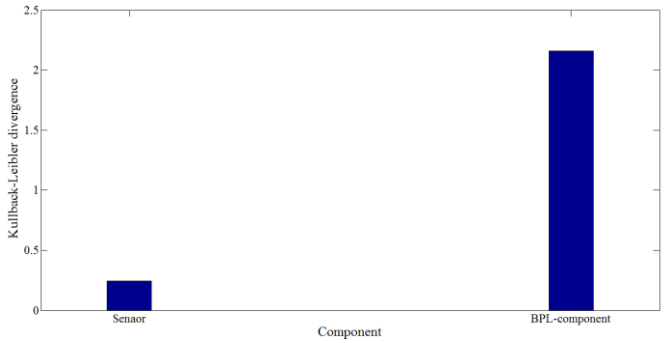


Figure 8. Kullback-Leibler divergence between the unreliability curve of the BPL module and of its embedded components

## 4 THE SYSTEM-LEVEL MSPM

The results of the SA performed in Section 3 point at RTD as deserving more efforts accurate modeling for the RPS unreliability estimation. A component-level MSPM approach is here developed to describe the RTD degradation-to-failure process. The resulting model can be integrated into a system-level MSPM of the RPS, to estimate the system failure probability accounting for both aging- and environmental-dependent transition rates of the RTD (thus, embedding more knowledge into the modeling of the most important contributor to the RPS unreliability). Results are compared with those from the RPS-MCM.

### *4.1 The RTD-MSPM*

Among the RTDs failure modes (e.g., bias, drift,

performance degradation, freezing and calibration error), experimental evidence suggests that the main failure mode is drift (Balaban et al., 2009). Drift is measured by the response time $\tau$ that the RTD needs to reach 63.2% of a sudden temperature change of the RTD. Aging $t$ and the air gap size $\delta$ between the bottom of the thermowell and the sensing tip (that changes because of contamination and mechanical shocks) are the most likely contributors to the drift (Hashemian, 2011). Therefore, the response time $\tau(t,\delta)$ is assumed not to exceed a RTD failure threshold $\gamma_Y$ during normal operation and the RTD failure boundary is defined as $\partial F = G(t,\delta) = 0$, where,

$$G(t,\delta) = \tau(t,\delta) - \gamma_Y \quad (4)$$

The RTD-MSPM shown in Figure 9 depicts, in a two-state diagram, the partition by $\partial F$ of the safe domain $S$ from the failure domain $F$ of the RTD. The RTD-MSPM assumptions are described as follows:

- $C_0^{RTD}$ is the RTD functioning state and $C_1^{RTD}$ is the RTD drift failure state.
- Transitions can occur between the two states with failure rate $\lambda_{(0,1)}^{RTD}(t,\delta)$ and repair rate $\mu_{(1,0)}^{RTD}(t,\delta)$, with respect to the aging time $t$ and the affecting factor $\delta$.
- At the initial time $t$=0, the RTD is in its initial functioning state $C_0^{RTD}$.

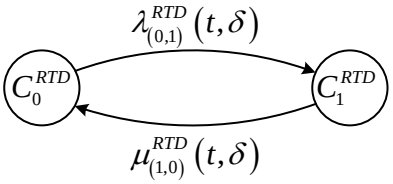


Figure 9. The RTD-MSPM model

To estimate the transition rates, we build the empirical relationship plotted in Figure 10 between $\tau$, $t$ and $\delta$ based on the experimental data listed in Tables 5 and 6 (Hashemian, 2011; Yun et al., 2012). For further details on the empirical model, the interested the reader may refer to (Wang et al., 2016).

Table 5. Experimental data for $\tau$ at fixed $t$ and $\delta$=0 (Yun et al., 2012)

| Aging time $t$ [yr] | Response time $\tau$ [s] |
|---|---|
| 0 | 2.1 |
| 2 | 4.4 |
| 4 | 4.8 |
| 5 | 5.0 |
| 6 | 5.2 |

Table 6. Experimental data for $\tau$ at $t$=0 and fixed $\delta$ (Hashemian, 2011; Yun et al., 2012)

| Air gap size $\delta$ [mm] | Response time $\tau$ [s] |
|---|---|
| 0 | 0.9 |
| 0 | 3.3 |
| 0.2 | 4.1 |
| 0.4 | 5.0 |
| 0.5 | 2.94 |
| 0.6 | 5.9 |
| 0.8 | 6.5 |
| 1.0 | 3.33 |
| 1.0 | 7.5 |
| 1.5 | 3.48 |
| 2.0 | 3.58 |

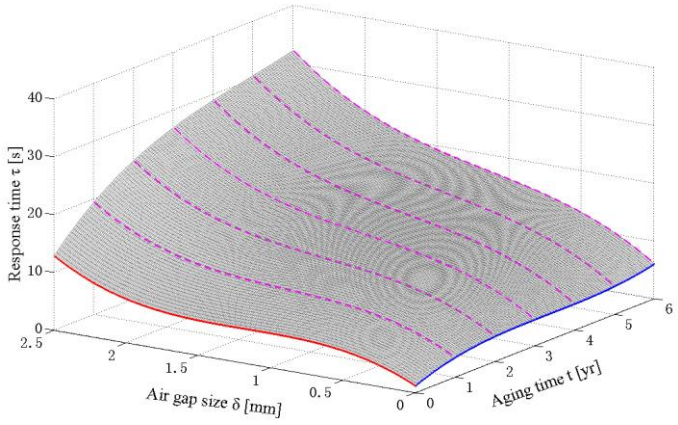


Figure 10. The empirical relationship $\tau(t,\delta)$

Monte Carlo (MC) simulation is used to simulate the stochastic evolution of $\tau$, when the relationship between $\tau$, $t$ and $\delta$ is taken as the one plotted in Figure 10. The cumulative distribution function (cdf) $P_S(t|\delta)$ can, thus, be estimated as the probability of $\tau(t,\delta)$ to exceed $\gamma_Y$ at a given time $t$, based on the batch of MC simulations that have been run.

Figures 11 and 12 show the $\lambda_S(t|\delta)$ and $P_S(t|\delta)$ obtained from RTD-MSPM, compared with $\lambda_S$ of Table 1 and $P_S(t)$ of the MCM of Figure 6. It is worth noticing that $\lambda_S(t|\delta)$ of Figure 11 shows the typical infant mortality and wear out periods, and tends to be constant in the RTD useful life, which coincides with a general bath-tub curve hypothesis. In Figure 12 the $P_S(t|\delta)$ is close to the $P_S(t)$ which, however, overestimates the unreliability of the RTD. The degradation process model in the MSPM is more realistic than in MCM, and on the other hand, the latter is not able to guarantee the drift onset beyond a threshold value (especially at low aging).

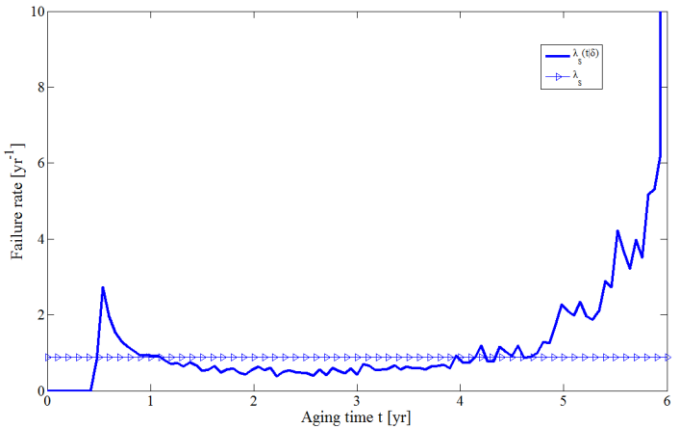


Figure 11. Time-dependent failure rate from RTD-MSPM and constant failure rate from database

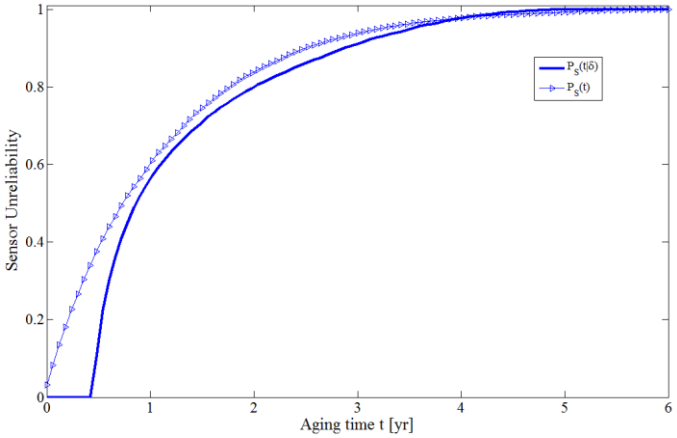


Figure 12. The cdfs from RTD-MSPM and from RTD-MCM

### *4.2 The system-level RPS-MSPM*

The system-level RPS-MSPM model of Figure 13 enriches the RPS-MCM model of Figure 2 by embedding the RTD-MSPM model of Figure 9, whereas components other than the RTD are assumed to obey binary behaviors as in the reference MCM. It is worth pointing out the use of $\lambda_S(t|\delta)$ as the aging- and environmental-dependent transition rate of the RTD from functioning state to any of the state of the diagram that entails its involvement (i.e., states 0 to 1, and 3 to 5).

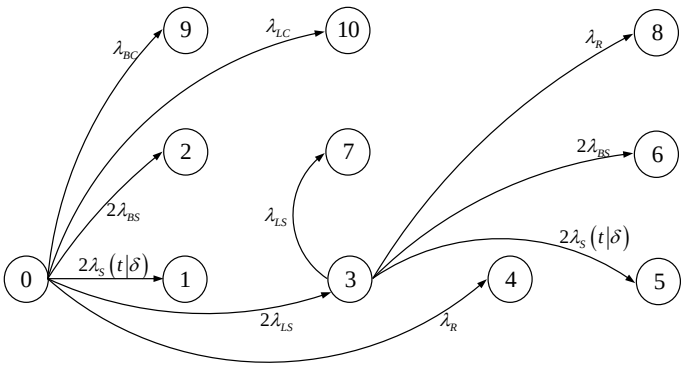


Figure 13. The system-level RPS-MSPM

The cdf $P(t|\delta)$ (i.e., the RPS system unreliability when aging and factors affecting the degradation of the RTD are considered) can be estimated by resorting to a two-loop MC simulation (Wang et al., 2016). In few words, the inner loop estimates the RTD failure time, by accounting for both stochastic (the air gap size between the sensing element tip and the thermowell bottom) and deterministic (the RTD age) processes, as described in Section 4.1, whereas the outer loop implements a crude direct Monte Carlo simulation (Zio, 2013) to build the $P(t|\delta)$, by sampling all the component failure times from the respective probability distributions.

Figure 14 shows the comparison between $P(t|\delta)$ of the RPS-MSPM and $P(t)$ of the RPS-MCM. With the integration of the MSPM of the most affecting component, overestimation of the system unreliability is reduced, so that over-conservatism of reactor design and over-demand of inspection and maintenance can be effectively avoided, especially at the early stage of the system life.

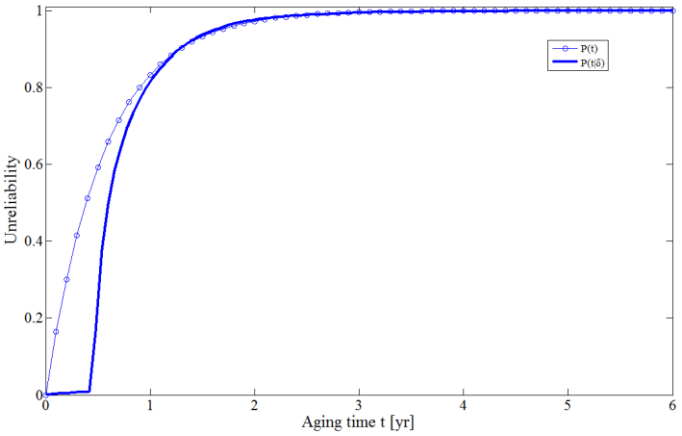


Figure 14. System unreliability curves of the RPS-MSPM and of the RPS-MCM

## 5 CONCLUSION

In this study, a SA has been performed to find the most important module and the most affecting component in the module. This provides the indication to the analyst of which components deserves more accurate modeling, according to their contribution to the system unreliability.

The case study shows that, once the most important component is identified, the additional modeling effort to build its component-level MSPM is paid back by the effective reduction of the overestimation of the system unreliability, compared to the MCM binary-states system-level modeling, supporting the system-level MSPM as an adequate model with controlled computation demand.

## 6 REFERENCE


Aldemir, T. 2013. A survey of dynamic methodologies for probabilistic safety assessment of nuclear power plants. *Annals of Nuclear Energy, 52, pp. 113-124.*

Balaban, E., Saxena, A., Bansal, P., Goebel, K. F. and Curran, S. 2009. Modeling, detection, and disambiguation of sensor faults for aerospace applications. *Sensors Journal, IEEE, No. 9(12), pp. 1907-1917.*

Baraldi, P., Di Maio, F., Genini, D. and Zio, E. 2015. Comparison of data-driven reconstruction methods for fault detection. *IEEE Transactions in reliability, Vol. 64, No. 3, pp. 852-860.*

Di Maio, F., Colli, D., Zio, E., Liu, T. and Tong, J. J. 2015. A Multi-State Physics Modeling approach for the reliability assessment of Nuclear Power Plants piping systems. *Annals of Nuclear Energy 80, pp. 151-165.*

Di Maio, F., Nicola, G., Zio, E. and Yu, Y. 2014. Ensemble-based sensitivity analysis of a Best Estimate Thermal Hydraulics model: Application to a Passive Containment Cooling System of an AP1000 Nuclear Power Plant. *Annals of Nuclear Energy 73, pp. 200-210.*

Diaconis, Persi, Zabell and Sandy, L. 1982. Updating subjective probability. *Journal of the American Statistical Association 77 (380), pp. 822–830.*

Gibbs, Alison L., Edward Su and Francis. 2002. On choosing and bounding probability metrics. *International Statistical Review 70 (3), 419–435.*

Hashemian, H. M. 2011. Measurement of Dynamic Temperatures and Pressures in Nuclear Power Plants. *Ph.D. Thesis.*

IAEA, 1992. Case study on the use of PSA methods: Assessment of technical specifications for the reactor protection system instrumentation. *IAEA-TECDOC-669.*

Kullback, S. and Leibler, R.A. 1951. On information and sufficiency. *Annals of Mathematical Statistics 22, pp. 79–86. http://dx.doi.org/10.1214/aoms/1177729694.*

Lin, Y. H., Li, Y. F. and Zio, E. 2015. Integrating Random Shocks into Multi-State Physics Models of Degradation Processes for Component Reliability Assessment. *Reliability, IEEE Transactions on Reliability 64, No. 1, pp. 154-166.*

US: EPRI, 2008. Utility requirement document annex a reliability data base for passive ALWR PRAs.

Wang, W., Di Maio, F. and Zio, E. 2016. Component- and System-Level Degradation Modeling of Digital Instrumentation and Control Systems Based on a Multi-State Physics Modeling Approach. *Submitted to Annals of Nuclear Energy.*

Wang, W., Zhao, J., Tong, J. J., Zhou, J. X. and Xiao, P. 2015. Evaluation Method of Reliability Indicator of Reactor Protection System. *Atomic Energy Science and Technology, 49 (6), pp. 1101-1108*.

Yun, D., Yacout, A. M. and Vilim, R. B. 2012. Modeling the Aging Effects of Nuclear Power Plant Resistance Temperature Detectors. *8th International Topical Meeting on Nuclear Plant Instrumentation, Control, and Human-Machine Interface Technologies 2012, NPIC and HMIT 2012: Enabling the Future of Nuclear Energy.*

Zio, E. 2013. The Monte Carlo simulation method for system reliability and risk analysis. *London: Springer.*

Zio, E. 2014. Integrated deterministic and probabilistic safety assessment: concepts, challenges, research directions. *Nuclear Engineering and Design, 280, pp. 413-419.*

Zio, E. 2016. Some challenges and opportunities in reliability engineering. *IEEE Transaction on Reliability*.